ELSEVIER

Journal of Hydrology 203 (1997) 109–118

Journal of Hydrology

Real-time tracking of convective rainfall properties using a two-dimensional advection–diffusion model

Akira Kawamura[a,*], Kenji Jinno[a], Ronny Berndtsson[b], Takashi Furukawa[a]

[a]*Department of Civil Engineering, Kyushu University, Fukuoka, Japan*
[b]*Department of Water Resources Engineering, Lund University, Lund, Sweden*

Received 18 March 1996; revised 20 January 1997; accepted 4 July 1997

Abstract

There is a need to improve rainfall forecasting capabilities for small ungaged urban catchments to reduce flooding hazards and pollution release. For this purpose, information is required on small-scale and short-term convective cell behavior. We use a two-dimensional stochastic advection–diffusion model to parameterize the space–time rainfall intensity from convective rainfall. The rainfall intensity resulting from different separable components of the rain cell, such as apparent turbulent diffusion and development/decay of rainfall intensity, is quantified for 10 observed and, for southern Sweden, representative high-intensity rainfall events. This is done following a Lagrangian approach. It is shown the used model was able to respond to rapid changes in observed rainfall intensity in both space and time, thus giving a small average root-mean-square error for all 10 events (0.06 mm min^{-1}). When dividing the total rainfall intensity into apparent turbulent diffusion and development/decay terms, respectively, it was shown that $D_{y,center}$ and γ_{center} contribute approximately equally to the observed rainfall intensity. The $D_{x,center}$ is usually only half the value of $D_{y,center}$, thus indicating less intensity contribution from this term and that the general elliptical shape of rain cells are elongated in the direction of movement. The observations indicate that the cumulus stage represents half and the dissipating stage half of the total cell development, respectively. The results can be used as first choice of parameter values when modeling rain cell movement over ungaged areas and the presented methodology can be used to study the effects of different cell components on total rainfall intensity. © 1997 Elsevier Science B.V.

Keywords: High-intensity rainfall; Real-time prediction

1. Introduction

There is a requirement to increase the accuracy of rainfall forecasting models for prediction of runoff in small urban ungaged catchments, and thus eventually to prevent flooding hazards. The time scale for prediction that these models should operate at is less than 1 h and with a typical space scale of a few square kilometers (see for example Berndtsson and Niemczynowicz, 1988; Schilling, 1990). Therefore, we may define the meso-γ scale (2–20 km; see Orlanski, 1975) as the rainfall fluctuation scale that is of main interest. The rainfall variation on this scale generally corresponds to the behavior of individual rain cells. To improve the forecasting accuracy, it is thus essential that the knowledge on convective cell behavior is expanded to improve the mathematical description in the models.

In general, most models for real-time control of hydrological systems use a stochastic description of

* Corresponding author.

PII S0022-1694(97)00088-7

the rainfall field (Georgakakos and Bras, 1984; Georgakakos and Hudlow, 1984; Georgakakos, 1986). Models for short-term rainfall forecasting or nowcasting in most cases use radar data as input (Bellon and Austin, 1984; Einfalt and Denoeux, 1987; Browning and Collier, 1989; French and Krajewski, 1994). However, many small urban catchments are still not equipped by radar. Instead, observations are often done by rain gages. Thus, there is a need to extend the use of rain gage data for rainfall forecasting. If radar data are also at hand, the radar can provide information on a larger scale embedding the rain gage system (e.g. by specifying boundary conditions for the forecasting area, see Burlando et al., 1996; Kawamura et al., 1997).

According to the above the present model builds on a joint conceptual and stochastic framework in which both rain gage and radar data may be included (Jinno et al., 1993). The model methodology can be used for real-time prediction of rainfall distribution on the aforementioned time- and space-scale. This methodology is based on a two-dimensional stochastic advection–diffusion equation in combination with a Fourier domain shape method (e.g. Kumar and Foufoula-Georgiou, 1990) and an extended Kalman filter algorithm (e.g. Bras and Rodriguez-Iturbe, 1985). It was shown that the model can be used to forecast motion, shape, size and intensity distribution of individual rain cells. Since a Fourier domain shape method is used to represent the rainfall field and the coupled Gaussian noise, the model domain, such as irregularly spaced rain gage networks, does not have to be discretized. The model can be included in an interactive management system for drainage since it uses a recursive estimation procedure for parameter identification.

In view of the above, the objective of the present paper is to use the aforementioned model methodology to study variability patterns of high-intensive convective rainfall events as observed in a dense rain gage network. In particular, we are interested in trying to separate the effects of advective velocity, apparent turbulent diffusion, and the development/decay of rainfall rate resulting from cell morphological changes on the overall rainfall intensity.

2. Theoretical considerations

Jinno et al. (1993) showed that a two-dimensional advection–diffusion equation is able to describe the observed rainfall intensity at ground level. In this model, it is assumed that during short time periods (minutes), the main forces acting on the rain cell are advection and diffusion. Indications that this assumption is relevant are the frequently found Gaussian-shaped spatial intensity pattern of individual rain cells (Sharon, 1972; Zawadzki, 1973; Marshall, 1980). The Gaussian function constitutes a particular solution to the advection–diffusion equation.

Using a Lagrangian view of the rainfall intensity field (moving along with the same speed as the rain cell), the Lagrangian derivative of a two-dimensional stochastic advection–diffusion equation may be expressed as (assuming a homogeneous rainfall field)

$$\frac{\mathrm{d}R(t)}{\mathrm{d}t}=\frac{\partial R(x,y,t)}{\partial t}+u\frac{\partial R(x,y,t)}{\partial x}$$
$$=D_x\frac{\partial^2 R(x,y,t)}{\partial x^2}+D_y\frac{\partial^2 R(x,y,t)}{\partial y^2}$$
$$-\gamma R(x,y,t)+\varepsilon(x,y,t) \quad (1)$$

where $R(x, y, t)$ is the rainfall intensity in time and space (m min^{-1}), u is the advective velocity of the rainfall cell in the direction of movement (m min^{-1}), D_x and D_y are the apparent diffusion coefficients in the x- and y-axis directions, respectively (m^2 min^{-1}), γ is the development/decay coefficient of the rainfall intensity (min^{-1}), and $\varepsilon(x, y, t)$ is a stochastic component with zero-mean Gaussian white noise in time and space (m min^{-2}).

The second-order partial differential [Eq. (1)] is transformed into a set of ordinary differential equations by applying a double Fourier series expansion. The rainfall field $R(x, y, t)$ and the coupled Gaussian white noise $\varepsilon(x, y, t)$ are expanded as

$$R(x,y,t)=\frac{A_{0,0}(t)}{2}+\sum_{m=1}^{M}\sum_{n=0}^{N}\left[A_{m,n}(t)\cos\mathbf{F}_1(x,y,m,n)\right.$$
$$\left.+B_{m,n}(t)\sin\mathbf{F}_1(x,y,m,n)\right]$$
$$+\sum_{m=0}^{M}\sum_{n=1}^{N}\left[C_{m,n}(t)\cos\mathbf{F}_2(x,y,m,n)\right.$$
$$\left.+D_{m,n}(t)\sin\mathbf{F}_2(x,y,m,n)\right] \quad (2)$$

$$\varepsilon(x,y,t)=\sum_{m=1}^{M}\sum_{n=1}^{N}\left[E_{m,n}(t)\cos\mathbf{F}_1(x,y,m,n)+F_{m,n}(t)\sin\mathbf{F}_1(x,y,m,n)+G_{m,n}(t)\cos\mathbf{F}_2(x,y,m,n)+H_{m,n}(t)\sin\mathbf{F}_2(x,y,m,n)\right] \quad (3)$$

where

$$\mathbf{F}_1(x,y,m,n)=\frac{2\pi mx}{\lambda_x}+\frac{2\pi ny}{\lambda_y} \quad (4)$$

$$\mathbf{F}_2(x,y,m,n)=\frac{2\pi mx}{\lambda_x}+\frac{2\pi ny}{\lambda_y} \quad (5)$$

In Eqs. (2)–(5), $A_{m,n}$, $B_{m,n}$, $C_{m,n}$, $D_{m,n}$, $E_{m,n}$, $F_{m,n}$, $G_{m,n}$ and $H_{m,n}$ are Fourier coefficients, M and N are the number of terms in the expansion procedure, and λ_x and λ_y are wave lengths for the x- and y-axis directions, respectively, that cover the entire area where rain gages are installed.

In the further analyses, we assume a position in the center of the rain cell (point with peak rainfall intensity) and a Lagrangian point of view (assuming movement along the x-axis) (see Kawamura et al., 1992). Consequently, we may define the diffusion terms and the development/decay term of Eq. (1) (the nonrandom right-hand terms) at this point according to

$$D_{x,\text{center}}=D_x\left.\frac{\partial^2 R(x,y,t)}{\partial x^2}\right|_{\substack{x=X_L(t)\\y=Y_L(t)}}$$

$$=D_x\sum_{m=1}^{M}\sum_{n=0}^{N}\left[-\left(\frac{2\pi m}{\lambda_x}\right)^2 A_{m,n}(t)\cos\mathbf{F}_1(x,y,m,n)-\left(\frac{2\pi m}{\lambda_x}\right)^2 B_{m,n}(t)\sin\mathbf{F}_1(x,y,m,n)\right]$$

$$+D_x\sum_{m=1}^{M}\sum_{n=1}^{N}\left[-\left(\frac{2\pi m}{\lambda_x}\right)^2 C_{m,n}(t)\cos\mathbf{F}_2(x,y,m,n)-\left(\frac{2\pi m}{\lambda_x}\right)^2 D_{m,n}(t)\sin\mathbf{F}_2(x,y,m,n)\right] \quad (6)$$

$$D_{y,\text{center}}=D_y\left.\frac{\partial^2 R(x,y,t)}{\partial y^2}\right|_{\substack{x=X_L(t)\\y=Y_L(t)}}$$

$$=D_y\sum_{m=1}^{M}\sum_{n=1}^{N}\left[-\left(\frac{2\pi n}{\lambda_y}\right)^2 A_{m,n}(t)\cos\mathbf{F}_1(x,y,m,n)-\left(\frac{2\pi n}{\lambda_y}\right)^2 B_{m,n}(t)\sin\mathbf{F}_1(x,y,m,n)\right]$$

$$+D_y\sum_{m=0}^{M}\sum_{n=1}^{N}\left[-\left(\frac{2\pi n}{\lambda_y}\right)^2 C_{m,n}(t)\cos\mathbf{F}_2(x,y,m,n)-\left(\frac{2\pi n}{\lambda_y}\right)^2 D_{m,n}(t)\sin\mathbf{F}_2(x,y,m,n)\right] \quad (7)$$

$$\gamma_{\text{center}}=\gamma R(x,y,t)\Big|_{\substack{x=X_L(t)\\y=Y_L(t)}} \quad (8)$$

where $X_L(t)$ and $Y_L(t)$ are the Lagrangian coordinates of the center of the cell with peak intensity. They are calculated as

$$X_L(t)=X_L(0)+\int_0^t u(\tau)\,d\tau \quad (9)$$

$$Y_L(t)=Y_L(0)+\int_0^t v(\tau)\,d\tau=Y_L(0) \quad (10)$$

where $u(\tau)$ and $v(\tau)$ are the mean velocities for the cell center in the x- and y-axis directions, respectively. The value of $v(\tau)$ is zero since this is taken in the direction of movement.

In the modeling below, parametrization is the same as made by Jinno et al. (1993). Consequently, here, parameter values are only described briefly, while Jinno et al. (1993) give more details on the specific parameter choice. The discrete time interval, Δt, was set to 0.1 min (one-tenth of the observation interval). To estimate initial parameter values for the Fourier coefficients, a Gaussian-shaped cell was generated using an initial cell strength corresponding to 500 m min^{-1} over a square area of 100 m^2. The initial location for this structure was chosen according to observed speed and wind direction. Wave lengths, λ_x and λ_y, were set to 30 000 and 10 000 m, respectively, and M and N were both set to 5. The system noise level (expressed as a percentage of the initial value for the physical parameters) was set to 5% for

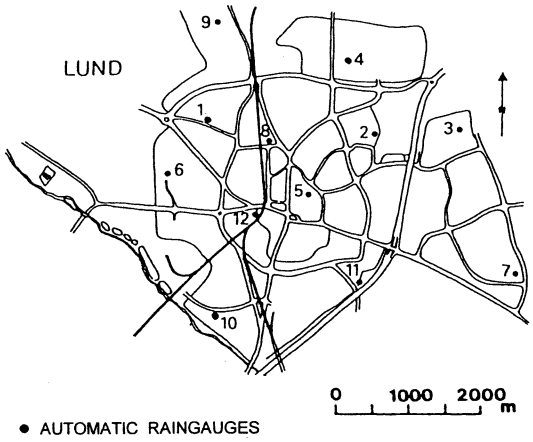

Fig. 1. Location of rain gage network (Niemczynowicz, 1984).

the four physical parameters (u, D_x, D_y, and γ). The system noise level for all Fourier coefficients [except $A_{0,0}(t)$, $A_{m,0}(t)$, $B_{m,0}(t)$, $C_{0,n}(t)$ and $D_{0,n}(t)$] was set to a constant value of 5% of the initial power spectrum for the most dominant wave numbers $[(A_{1,1}(0)^2 + B_{1,1}(0)^2 + C_{1,1}(0)^2 + D_{1,1}(0)^2)/4]$ put uniformly over the power spectrum for the system noise. Further theoretical and practical details on the above modeling approach for real-time prediction of small-scale rainfall are given by Jinno et al. (1993).

Eqs. (6)–(10) can be used to obtain a physical description of the behavior of convective rainfall. Using the Lagrangian approach and an assumed position in the center of the rain cell we may analyze the turbulent flow field as indicated by the two-dimensional flux of rainfall at ground level. The terms $D_{x,\text{center}}$ and $D_{y,\text{center}}$ quantify how much of the rainfall intensity that accounts for apparent turbulent diffusion and similarly, the term γ_{center} gives the effect of development/decay. The values of $D_{x,\text{center}}$ and $D_{y,\text{center}}$ should be interpreted as the change in the shape of the cell center with time in the x- and y-axis directions, respectively. Negative values mean that the shape is convex (peak in rainfall intensity). Similarly, positive values indicate a concave shape (depression in the rainfall intensity field) and that the coordinate center is no longer located in the center of the cell. The term γ_{center} similarly indicates the development/decay (sink/source) of the cell center. Generally speaking, positive values of γ_{center} mean a decaying rainfall intensity behavior for the cell. Similarly, negative values mean that the cell is growing or developing in rainfall intensity. However, note that actual rainfall intensity development at the center of the rain cell is also affected by $D_{x,\text{center}}$ and $D_{y,\text{center}}$ contributions as expressed in Eq. (1).

3. Investigated rainfall events

We used 10 high-intensive rainfall events observed by Niemczynowicz (1984) to quantify the effects of advective velocity, apparent turbulent diffusion and development/decay on the overall rainfall intensity. The observations were done in a 12-gage (tipping-bucket gages with a resolution of 0.035 mm min^{-1}), 25 km^2 catchment (see Fig. 1). The observation period was from June 1978 to September 1980.

The rainfall data in this paper were selected from the 10 high-intensive rainfall events initially analyzed by Niemczynowicz and Jönsson (1981) and Berndtsson et al. (1994). The time span for the data analyzed by Niemczynowicz and Jönsson (1981) and Berndtsson et al. (1994) was 60 min and several rain cells were included in each of these 60 min events. In this paper, however, spatial plots for every time step (every minute) in the 10–60 min data base were manually examined and 10 shorter periods with clear properties of a single rain cell moving over the catchment were selected. The duration for these shorter single-cell events varied from 11 to 41 min (see Table 1). Consequently, the data used were examined in detail and only sequences of data for which the overall quality could be ensured were included in the study.

All events were typical convective rain storms that appear over the area. The most common meteorological situation bringing convective rainfall to the south of Sweden is after the passage of cold fronts, especially when the low-pressure area is to the north and the air masses move from south to north (Niemczynowicz and Jönsson, 1981). Events 2, 3 and 4 in Table 1 are observations from such meteorological conditions. Events 1 and 5–10 are from another common meteorological situation resulting in convective rainfall: when no frontal structures appear but westerly winds bring wet air masses that rise to cumulonimbus clouds. This situation results in short and the most high-intensity rainfall over the observation area. The gaged area is predominantly

Table 1
Intensity characteristics and identified final parameters of Eq. (1) for the 10 high-intensive rainfall events

Rainfallevent	Duration (min)	Observed maximum intensity (mm min^{-1})	u (m min^{-1})	$D_x \times 10^4$ (m^2 min^{-1})	$D_y \times 10^4$ (m^2 min^{-1})	$\gamma \times 10^{-2}$ (min^{-1})	$\gamma_{min} \times 10^{-2}$ (min^{-1})	Model error (mm min^{-1})
1	19	1.5	290	1.4	0.93	1.8	0.63	0.08
2	36	2.2	490	4.1	3.3	4.0	0.00	0.06
3	21	1.7	0	2.3	1.5	2.5	0.50	0.07
4	19	1.3	300	1.6	0.85	1.7	1.20	0.04
5	16	2.2	500	2.4	1.3	2.6	0.20	0.06
6	13	2.1	230	1.5	1.0	1.4	0.40	0.07
7	11	0.8	640	0.68	0.34	0.67	0.27	0.04
8	41	2.4	280	5.0	2.9	4.7	-0.40	0.05
9	12	1.0	510	1.4	0.76	1.4	0.97	0.05
10	18	1.4	190	1.1	0.87	1.2	0.08	0.03
Mean	21	1.7	343	2.15	1.38	2.20	0.39	0.06
Standard deviation	10	0.6	190	1.38	0.96	1.28	0.47	0.02

flat, but with a marked gradient from southwest to northeast (20–70 m a.m.s.l.). This results in an increasing annual precipitation of about 35 mm $year^{-1}$ km^{-1} to the northeast direction. However, the topographical trend is hardly seen in individual convective events.

Table 1 gives a further description of the 10 short-term analyzed rainfall events. As is seen from the table, the maximum observed rainfall intensity varies from 0.8 to 2.4 mm min^{-1}. This roughly corresponds to return periods of 10–15 years for the actual area (Niemczynowicz, 1984). All events were recorded during the summer period when localized convection is the dominant rainfall mechanism. The duration of the analyzed events varied between 11 and 41 min and typically displayed a confined zone of high-intensive rainfall moving over the catchment. It can therefore be assumed that the chosen convective events correspond to the behavior of individual rain cells. For all events, 1 min data from 10 to 12 rain gages were used.

Table 1 also gives the identified final parameter values of Eq. (1). From the model error it is seen that the uncertainty (calculated as the root-mean-square error between observed and modeled values for all gages and the entire simulation period) in general is very small (average of 0.06 mm min^{-1}), and thus the model is able to adapt to the very rapid and fluctuating rainfall intensities.

The average speed of the convective rainfall was identified to be 343 m min^{-1} ($u = 5.7$ m s^{-1}; Kawamura et al., 1996). The diffusion coefficient in the x-axis direction (direction of movement) is consistently larger ($D_x = 2.15 \times 10^4$ m^2 min^{-1}) than the one in the y-axis direction ($D_y = 1.38 \times 10^4$ m^2 min^{-1}). This is physically reasonable because of induced larger diffusion in the direction of movement. An elongation of the cells in the direction of movement is also often observed in experimental studies (see for example Berndtsson et al., 1994). Below we use the rainfall events in Table 1 to quantify properties of convective rainfall in terms of apparent turbulent diffusion and development/decay of rainfall intensity.

4. Properties of convective rainfall

The model has previously been tested and validated by Kawamura et al. (1992), Jinno et al. (1993) and Desa et al. (1997). The model was shown to behave in a consistent way and to give better results than, for example, pure translation of the rainfall field. The sensitivity of the model was also checked by test runs for different choices of wave lengths λ_x, λ_y, and number of terms in the Fourier series expansion. It was found that the prediction performance is not significantly affected by the choice of wave lengths. This is because the Fourier coefficients compensate each other and the variation in the physical parameters

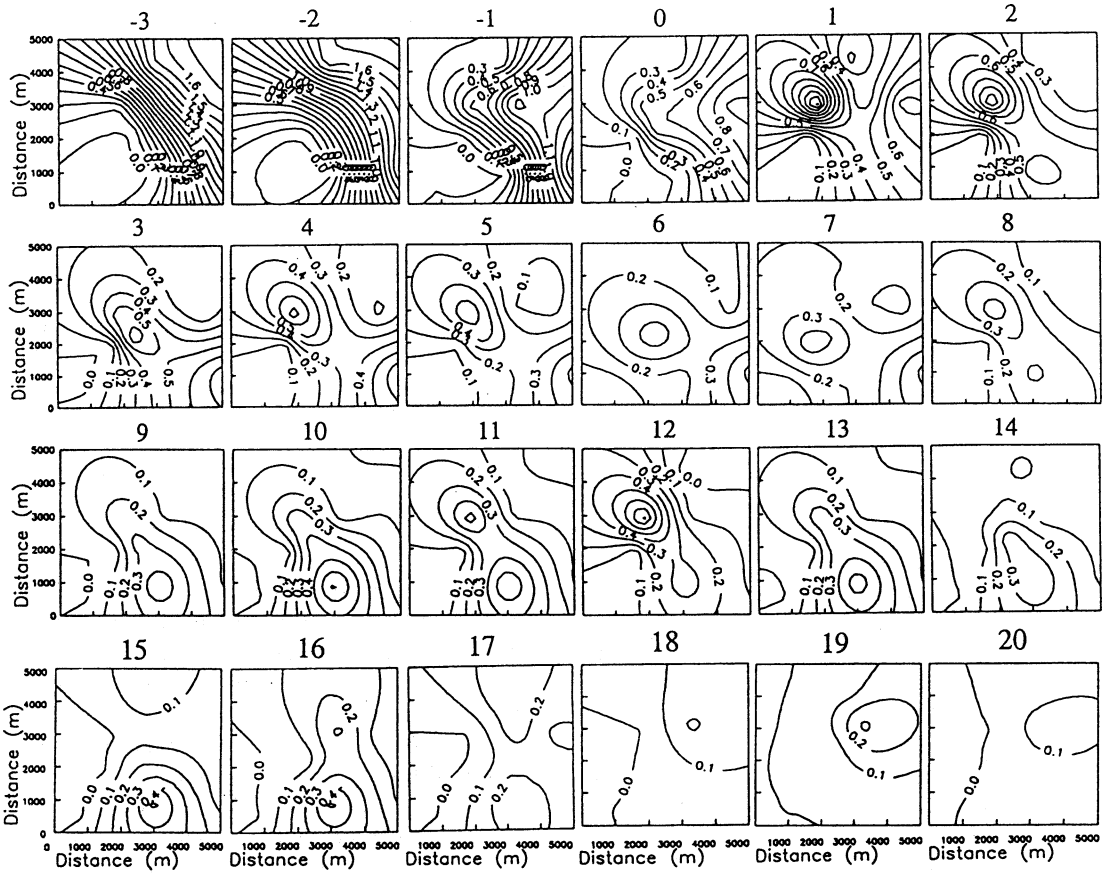

Fig. 2. Example of spatial intensity patterns over the tipping-bucket gage network during 24 min (event 1 in Table 1) (interpolation by kriging; mm min^{-1}).

tends to be more dependent on the system noise level. The model can at present be run on a standard PC.

Physical interpretation of observed rainfall variability is important to understand small-scale variations and ultimately to improve model efficiency. In this study, we use the nonrandom right-hand side terms of Eq. (1) to infer physical properties of convective rainfall. Consequently, we use a Lagrangian approach for tracking the diffusion terms and the development/decay term, Eqs. (6)–(10). For the description of the rain cells, we use the identified parameter values shown in Table 1.

Fig. 2 shows a typical example of spatial intensity patterns passing over the observation area (event 1 in Table 1; interpolation was done by kriging). Several cell-shaped intensity patterns are seen to move over the gaging network during the observation period. These are also seen in Fig. 3 which shows observed typical rainfall at one of the rain gages (event 1 in Table 1 for gage 8 in Fig. 1). Two clear intensity maxima are apparently passing over the rain gage during the 20 min period (corresponding to time step 0–20 min in Fig. 2). These maxima were interpreted as two separate rain cell structures that pass over the rain gage network.

Fig. 4 shows the corresponding calculated values of the rainfall intensity terms $D_{x,\mathrm{center}}$, $D_{y,\mathrm{center}}$ and γ_{center}. The identified cell structure 1 has large negative values of $D_{y,\mathrm{center}}$ and γ_{center} from the beginning of the identification procedure. This means that the

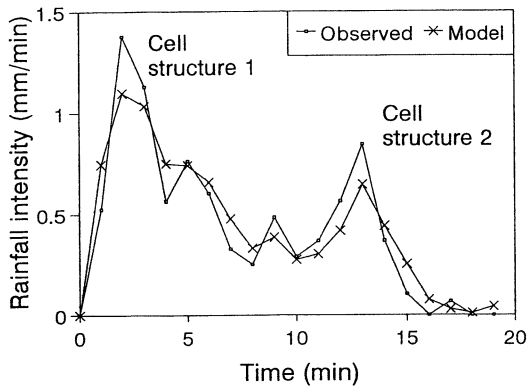

Fig. 3. Example of time series of observed rainfall at one of the rain gages during event 1 in Table 1 (see Fig. 2).

convex shape of the rainfall intensity field at the center of the cell is markedly peaked in the y-axis direction in the beginning of the observation period. On the other hand, the large negative γ_{center} means that the development/decay term is large in comparison to the diffusion term in the x-axis direction and that there is a large contribution from the γ_{center} term to the total rainfall intensity at ground level. In physical terms, this may be interpreted as a situation when the cell develops or expands (cumulus stage), but the actual rainfall intensity development at the center of the rain cell is determined by the total contribution of $D_{x,center}$, $D_{y,center}$ and γ_{center}. In this case, the total effect of diffusion by $D_{x,center}$ and $D_{y,center}$ is larger than that of cell development by γ_{center}, as indicated in Fig. 4, resulting in a virtual decrease of rainfall intensity at the cell center as shown in Fig. 2.

All intensity components gradually flatten out and approach constant small values (a flat intensity field) up to about 12 min from start. This means that the intensity gradually decreases (cf. Fig. 3) and that the cell reaches a dissipating stage. After about 12 min, however, the second cell structure starts to influence the parameter values and again there is drastic drop in the intensity terms (less for $D_{x,center}$). This means that again the intensity increases and a new cell starts to develop. This is seen in Fig. 3 as the second cell structure.

The occasional positive values for $D_{x,center}$ indicate that the x-axis coordinate center is no longer located in the location of the peak rainfall intensity (positive values indicating a concave intensity field). This is interpreted as effects of the second cell structure that now carries the peak intensity at some distance from the first cell center location.

Table 2 summarizes average descriptive statistics for the intensity components $D_{x,center}$, $D_{y,center}$ and γ_{center} for the 10 rainfall events in Table 1. From the table it is seen that average $D_{x,center}$ usually is only half the value of $D_{y,center}$. This means that the convex shape

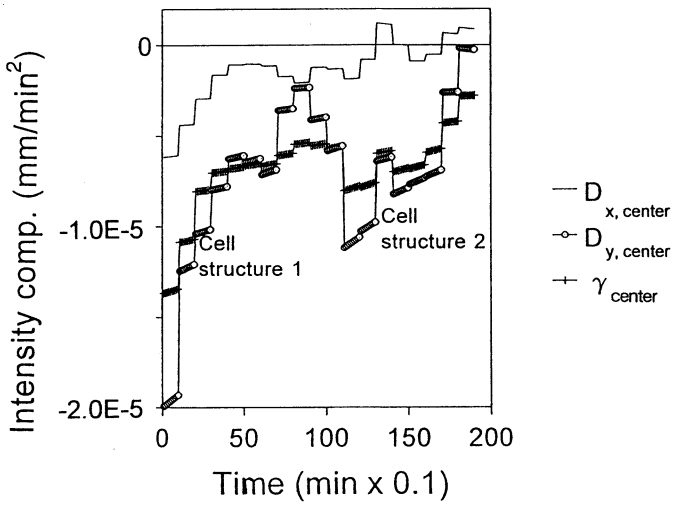

Fig. 4. Example of temporal evolution of the rainfall intensity components $D_{x,center}$ and $D_{y,center}$ (apparent turbulent diffusion term in the x- and y-axis directions, respectively) and γ_{center} (development/decay term) for the rainfall event shown in Figs. 2 and 3.

Table 2
Descriptive statistics for average intensity components $D_{x,center}$, $D_{y,center}$ and γ_{center} of the 10 rainfall events in Table 1 ($\times 10^7$, mm min^{-2})

	$D_{x,center}$	$D_{y,center}$	γ_{center}
Mean	−32.3	−74.6	−72.3
Standard deviation	36.7	103.0	52.9
Minimum	−115.0	−294.0	−187.0
Maximum	46.8	162.0	55.7

of the rainfall intensity field is markedly peaked in the y-axis direction, indicating a general elliptical shape of the rain cell elongated in the direction of movement. Average means of γ_{center} and $D_{y,center}$ are of the same order of magnitude, indicating that they contribute similarly to the rainfall intensity.

Fig. 5 shows time series of average values of calculated rainfall intensity components after cell identification for all 10 events. The averaging simply means taking the arithmetic average of the cell intensity components for each time step. The assumption behind the averaging is that the birth time of individual cells is close to the start of initial identification time for the cells in the calculation procedure. This implies an uncertainty for the interpretation of results since no information is at hand for the cell development outside the gaged area. However, the averaging may give general characteristics of the rainfall process over a gaged catchment of the actual size, because we ascertained that the time-development process of calculated rainfall intensity components after cell identification makes little difference for any of the 10 rainfall events of the catchment from the Lagrangian point of view, even though the advective velocity of rainfall cell varies as shown in Table 1. Consequently, the results may be viewed as average rain cell properties over a catchment area of 25 km^2 in size.

From Fig. 5, the general properties for all the investigated rainfall events are large negative values for both apparent turbulent diffusion (however, these are larger in the y-axis direction) and development/decay term in the early cell development stage (just after a cell has been identified). After cell identification, the negative terms increase towards almost constant values close to zero or small positive values. The development during the first stage (rapid increase in intensity) represents about half the total identified life time of the cell, while the other half represents the decaying stage. These two stages may indicate the cumulus stage and the dissipating stage of cell development, respectively.

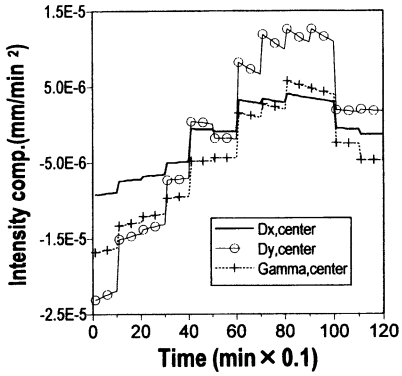

Fig. 5. Temporal evolution of average rainfall intensity components $D_{x,center}$ and $D_{y,center}$ (apparent turbulent diffusion term in the x- and y-axis directions, respectively) and γ_{center} (development/decay term) for the rainfall events summarized in Table 2.

5. Summary and discussion

In the present paper we have developed a methodology to separate and quantify different components of convective rainfall such as apparent diffusion and development/decay resulting from cell morphological changes. Using a Lagrangian approach the methodology was applied to 10 observed high-intensive short-term rainfall events.

It was shown the used model was able to respond to rapid changes in observed rainfall intensity in both space and time, thus giving a small average root-mean-square error for all 10 events (0.06 mm min^{-1}). When dividing the total rainfall intensity into apparent turbulent diffusion and development/decay terms, respectively, it was shown that $D_{y,center}$ and γ_{center} contribute approximately equally to the observed rainfall intensity. The $D_{x,center}$ usually is only half the value of $D_{y,center}$, thus indicating less intensity contributions from this term and that the cells are typically elongated in the direction of movement. The observations indicate that the cumulus

stage represents half and the dissipating stage half of the total cell development, respectively.

A model like the one described has many potential uses. It can, in addition to practical real-time forecasting applications, also be used to parameterize the variation of rainfall structures. This, however, relies on the inherent assumption that the governing equations are physically sound and that the parameter values in the model reflect physically based properties of the actual rainfall process. If so, the model parameters can be conveniently used to describe the variability pattern of observed rainfall in terms of physically definable characteristics. This, in turn, may be practically utilized, e.g. when choosing model parameters for ungaged areas or when studying effects of parameter variability on the rainfall intensity in numerical studies.

The results of this study may be practically utilized when choosing initial parameter values of the presented model. The overall methodology can be used to further study and to parameterize small-scale rainfall variability. In most urban areas radar data are still not available on a sufficiently small scale to model individual cells. However, in areas, where radar is installed these data may provide valuable information on larger-scale movement and thus be used as, for example, boundary conditions for the proposed methodology (see Cluckie and Collier, 1991; Burlando et al., 1996).

The present methodology builds on the assumption that the birth time of the individual cells is close to the start of initial identification time for the cells in the calculation procedure. This implies an uncertainty for the interpretation of results since no information is at hand for the cell development outside the gaged area. The present methodology could therefore be strengthened by using radar data in combination wih rain gage observations. The radar data could be used to give a more accurate cell birth time to be combined with the calculation procedure which builds on rain gage observations.

Acknowledgements

This cooperative study was supported by the Scandinavia–Japan Sasakawa Foundation and the Swedish Natural Science Research Council.

References

Bellon, A., Austin, G.L., 1984. The accuracy of short-term radar rainfall forecast, Journal of Hydrology, 70, 35–49.

Berndtsson, R., Niemczynowicz, J., 1988. Spatial and temporal scales in rainfall analysis: some aspects and future perspectives, Journal of Hydrology, 100, 293–313.

Berndtsson, R., Jinno, K., Kawamura, A., Larson, M., Niemczynowicz, J., 1994. Some Eulerian and Lagrangian statistical properties of rainfall at small space–time scales, Journal of Hydrology, 153, 339–356.

Bras, R.L., Rodriguez-Iturbe, I., 1985. Random Functions and Hydrology. Addison-Wesley, Reading, MA, pp. 1–559.

Browning, K.A., Collier, C.G., 1989. Nowcasting of precipitation systems, Review of Geophysics, 27, 345–370.

Burlando, P., Montanari, A., Ranzi, R., 1996. Forecasting of storm rainfall by combined use of radar, rain gages and linear models, Atmospheric Research, 42, 199–216.

Cluckie, I.D., Collier, C.G. (Eds.), 1991. Hydrological Applications of Weather Radar. Ellis Horwood, New York, pp. 1–644.

Desa, M.M.N., Berndtsson, R., Niemczynowicz, J., 1997. Application of a two-dimensional advection diffusion model to urban rainfall prediction in Kuala Lumpur. Journal of Hydrology, (submitted manuscript).

Einfalt, T., Denoeux, T., 1987. Radar rainfall forecasting for real-time control of a sewer system. In: Yen, B.C. (Ed.), Urban Drainage. Hydraulics and Hydrology, Proceedings of the Fourth International Conference on Urban Storm Drains, Lausanne, 31 August–4 September, 1987, IAHR, Lausanne, pp. 47–48.

French, M.N., Krajewski, W.F., 1994. A model for real-time quantitative rainfall forecasting using remote sensing, 1. Formulation, Water Resources Research, 30, 1075–1083.

Georgakakos, K.P., 1986. A generalized stochastic hydrometeorological model for flood and flash-flood forecasting, 1. Formulation, Water Resources Research, 22, 2083–2095.

Georgakakos, K.P., Bras, R.L., 1984. A hydrologically useful station precipitation model, 1. Formulation, Water Resources Research, 20, 1585–1596.

Georgakakos, K.P., Hudlow, M.D., 1984. Quantitative precipitation forecast techniques for use in hydrological forecasting, Bulletin of the American Meteorological Society, 65, 1186–1200.

Jinno, K., Kawamura, A., Berndtsson, R., Larson, M., Niemczynowicz, J., 1993. Real-time rainfall prediction at small space–time scales using a two-dimensional stochastic advection–diffusion model, Water Resources Research, 29, 1489–1504.

Kawamura, A., Jinno, K., Berndtsson, R., 1992. Real-time prediction of urban-scale rainfall by use of a two-dimensional stochastic convection–diffusion model. In Proceedings of the Sixth IAHR International Symposium on Stochastic Hydraulics, 18-20 May, 1992, Taipei, pp. 751–758.

Kawamura, A., Jinno, K., Berndtsson, R., Furukawa, T., 1996. Parameterization of rain cell properties using an advection–diffusion model and rain gage data, Atmospheric Research, 42, 67–73.

Kawamura, A., Jinno, K., Furukawa, T., Wakimizu, K., Nishiyama, K., 1997. Study on characteristics of radar parameters and real-time prediction of ground rainfall, Journal of Japanese Society of Civil Engineers, 558 (II38), 31–43. (in Japanese with English abstract).

Kumar, P., Foufoula-Georgiou, E., 1990. Fourier domain shape analysis methods: a brief review and an illustrative application to rainfall area evolution, Water Resources Research, 26, 2219–2227.

Marshall, R.J., 1980. The estimation and distribution of storm movement and storm structures, using a correlation analysis technique and rain-gage data, Journal of Hydrology, 48, 19–31.

Niemczynowicz, J., Jönsson, O., 1981. Extreme rainfall events in Lund 1979–1980. Nordic Hydrology, 12, 129–142.

Niemczynowicz, J., 1984. An investigation of the areal and dynamic properties of short-term rainfall and its influence on runoff generating processes. D.Sc. Thesis, Department of Water Resources Engineering, Lund Institute of Science and Technogy, University of Lund, Lund, Report 1005, pp. 1–215.

Orlanski, I., 1975. A rational subdivision of scales for atmospheric processes, Bulletin of the American Meteorological Society, 6, 527–530.

Schilling, W., 1990. Rainfall data for urban hydrology: what do we need? In Niemczynowicz, J. (Ed.), Proceedings of the International Workshop on Urban Rainfall and Meteorology, St Moritz, Switzerland, 2–5 December 1990, pp. 13–38.

Sharon, D., 1972. The spottiness of rainfall in a desert area, Journal of Hydrology, 17, 161–175.

Zawadzki, I.I., 1973. Statistical properties of precipitation patterns, Journal of Applied Meteorology, 12, 459–472.